U.S. Department of Transportation
Federal Aviation Administration

Open Rotor Engine Aeroacoustic Technology Final Report

Continuous Lower Energy, Emissions and Noise (CLEEN) Program

Submitted by General Electric

DOT/FAA/AEE/2014-03

The Continuous Lower Energy, Emissions and Noise (CLEEN) Program is a Federal Aviation Administration NextGen effort to accelerate development of environmentally promising aircraft technologies and sustainable alternative fuels. The CLEEN Program is managed by the FAA's Office of Environment and Energy.

The report presented herein is the final report deliverable submitted by General Electric for a project conducted under the CLEEN Program to mature open rotor engine aeroacoustic design. This project was conducted under FAA other transaction agreement (OTA) DTFAWA-10-C-00046. This is report is report number DOT/FAA/AEE/2014-04 by the FAA's Office of Environment and Energy.

GENERAL ELECTRIC COMPANY

FAA CLEEN PROGRAM
OPEN ROTOR AEROACOUSTIC TECHNOLOGY
NON-PROPRIETARY REPORT

GE Aviation, One Neumann Way, Evendale, OH 45215

May 2013

S. Arif Khalid, David Lurie, Andrew Breeze-Stringfellow[1]
Trevor Wood, Kishore Ramakrishnan, Umesh Paliath[2]
John Wojno, Bangalore Janardan, Trevor Goerig[3]
Anthony Opalski[4]

Jack Barrett[5]

Prepared for Rhett Jefferies[6]

[1] GE Aviation – Fan & Compressor Aero Design
[2] GE Global Research – Aerodynamics & Acoustics Laboratory
[3] GE Aviation – Acoustics & Installation Aerodynamics
[4] GE Aviation – Aero Technology Laboratory
[5] GE CLEEN Program Manager
[6] FAA CLEEN Program Manager

Table of Contents

CHAPTER 1. SUMMARY

Building upon the successes of the UDF® program in the 1980's, open rotor designs for high flight speed efficiency and low community noise have been developed at GE in collaboration with NASA and the FAA. Targeting a narrow body aircraft with 0.78 cruise Mach number, the cost-share program leveraged computational fluid dynamics (CFD), computational aero-acoustics (CAA), and rig scale testing to generate designs that achieved significant noise reductions well beyond what was attained in the 1980's while substantially retaining cruise performance. This paper presents overall propeller net efficiency and acoustic assessments of GE's modern open rotor designs based on measured rig data and the progression of the technology from the 1980's through the present. Also discussed are the effects of aft rotor clipping, inter-rotor spacing, and disk loading. This paper shows how the two-phase design and scale model wind tunnel test program allowed for test results of the first design phase to feed back into the second design phase, resulting in 2-3% improvement in overall propeller net efficiency than the best efficiency design of the 1980's while nominally achieving 15-17 EPNdB noise margin to Chapter 4 (when projected to full scale for a prescribed aircraft trajectory and installation). Accounting for trades and near term advancements, such a propulsion system is projected to meet the goal of 26% fuel burn reduction relative to CFM56-7B powered narrow body aircraft.

CHAPTER 2. BACKGROUND AND GOALS

Section 2.1: Introduction

Concerns about fuel prices, energy security, and the environment are driving the pursuit of game-changing technologies for reductions in fuel burn and emissions while providing significant noise reductions relative to today's aircraft. The open rotor engine, consisting of dual counter-rotating propellers driven by a gas turbine core can deliver a step-change reduction in fuel burn compared to modern turbofan engines due to the lower fan pressure ratio that can be achieved. However, the noise that was inherent in open rotor designs that were examined in the 1980's (contemporary terms were "unducted fan" and propfan) presented a certification risk for such a propulsion system. GE, in cooperation with NASA and with FAA cost-share support, completed a two-phase, five-year technology maturation program consisting of rig scale design along with performance and acoustic wind tunnel testing that demonstrated substantial reductions in fuel burn with comparable acoustics to advanced turbofans.

After discussing background and goals, experimental setup, analysis methodology, and design features, this report describes the results, with an emphasis on how the aerodynamic performance was affected by the acoustic design features. As such, experimental trends of overall net efficiency make up the bulk of the results presented. Although acoustic measurements such as spectral power level or third octave band noise data are not presented here, the acoustic results shown below were obtained from model scale experimental data and projected to full-scale to assess performance relative to the program noise goals.

Section 2.2: Historic UDF® Program

In the 1980's GE helped develop the concept of open rotor propulsion. It was a comprehensive technology development program, of historic scale. As shown in Figure 1, the initial proof-of-concept testing under the original UDF® program consisted of three phases: an extensive scale model technology development phase (Hoff, 1990), which culminated in 2500 hours of model scale testing; followed by the development of a prototype engine, which was ground tested in 1985 (162 hours of testing); then flight test on two separate aircraft demonstrators, the Boeing 727-100 (Harris and Cuthbertson, 1987) and the McDonnell-Douglas MD-80 (Nichols, 1988), for a total of 281 hours of flight testing.

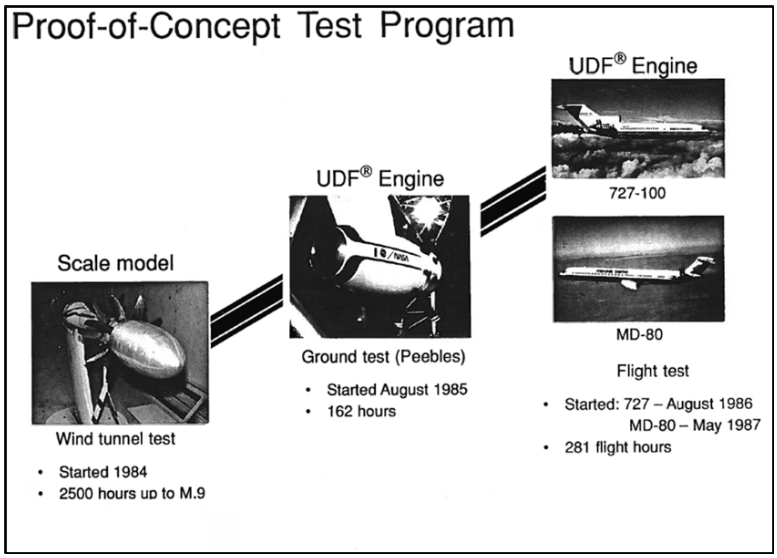

Figure 1: Historic 1980's UDF® demonstrator program.

To support such extensive model-scale technology testing, three Model-scale Propulsion Simulator (MPS) rigs were designed and fabricated: A vertically stacked rig (see Figure 2), which was developed for GE's Cell 41 Test Facility (MPS SN002); and two conventional, horizontally-oriented rigs, which were fabricated for Boeing and NASA (MPS SN001 and SN003). As illustrated in Figure 3, model scale testing was performed in a number of test facilities, including: GE Cell 41; NASA Glenn 9x15 Low Speed Wind Tunnel; NASA Glenn 8x6 High Speed Wind Tunnel; the Boeing Transonic Wind Tunnel (BTWT); and the acoustic wind tunnel at DNW. The objective of this extensive testing was to develop detailed physical understanding of open rotor aerodynamic performance and acoustics. Accomplishing this involved multiple efforts, including: assessing reference design levels for comparison to later flight test data; identifying noise source mechanisms; evaluating the effects of blade design parameters on aero performance and noise; and exploring noise reduction concepts, as noise was quickly identified as a challenge, with all acoustic modes cut-on and radiating.

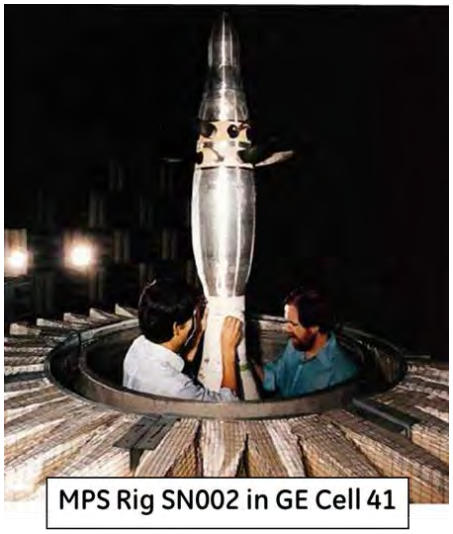

Figure 2: GE Cell 41 model-scale open rotor rig.

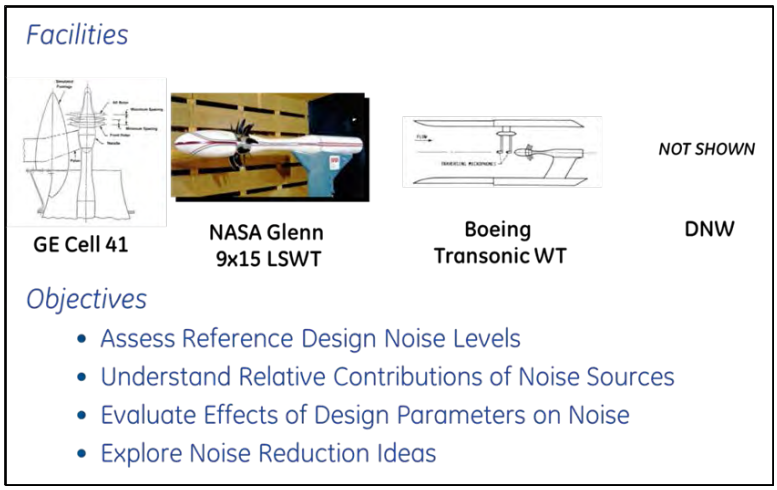

Figure 3: 1980's model-scale open rotor technology development program.

One key benefit of the extensive 1980's testing, was the verification of scalability of model scale results to the full-scale application. Through the UDF® program open rotor performance and acoustics were measured for the flight demonstrator blade design (F7A7), from model-scale all the way through the flight demonstrations. Comparisons between corresponding model scale and full scale data demonstrated that the model scale data could effectively projected to estimate full-scale results, as shown in Figure 4. These data comparisons, which were originally presented in 1988, show good comparisons on both a spectral level, as well as the Tone-Corrected Perceived Noise Level (PNLT), which is integrated to assess the Effective Perceived Noise Level (EPNL) community noise metric. In the upper right portion of Figure 4, the data comparisons show good agreement between the EPNL differences associated with early changes in blade count (8x8 vs. 10x8), based on the model scale results, and those actually measured during the flight test program. This scalability was central to the Open Rotor Aeroacoustic Technology Development portion of the FAA CLEEN program as it provided a basis for performing the technology development at model scale on the refurbished NASA rig, and projecting these results to full-scale using validated tools and methods.

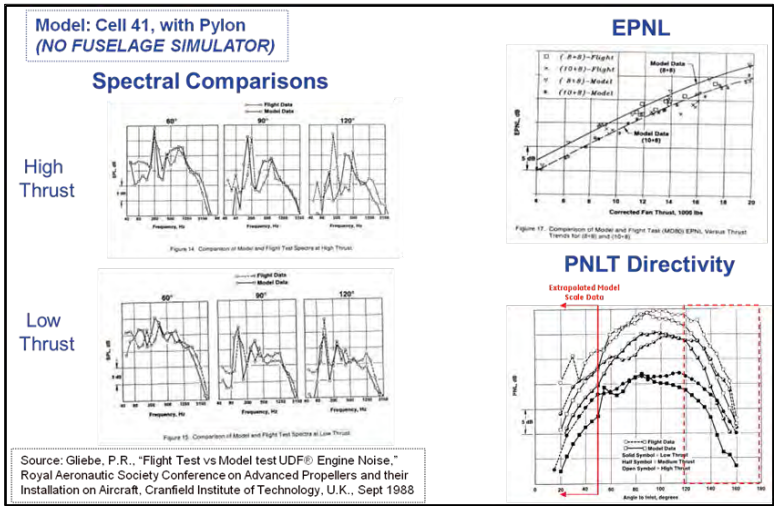

Figure 4: Scalability of model-scale results based on UDF® flight test data.

Even today, the UDF® program is still remembered within the community because it was a revolutionary concept in aero propulsion, and because the flight test demonstrator was very loud. However, this was not the full story, even in the 1980's, as shown below. Furthermore, the extensive testing identified the following noise mitigation strategies:

- Aeroacoustic blade design/geometry
- Blade operational pitch/speed optimization
- Increased blade counts
- Reduced disk loading
- Rotor-to-rotor spacing optimization
- Aft rotor clipping
- Increased pylon-to-rotor spacing
- Pylon wake mitigation

These strategies were leveraged for the GE36 product design, and provided the initial understanding used to develop the Gen1 designs under the Modern Open Rotor Aeroacoustic Technology Development effort under the FAA CLEEN Program.

Section 2.3: GE36 Product Program

In addition to the extensive technology development efforts under the original UDF® program, which were well documented in trade journals and external publications by GE, NASA and Boeing; in the late 1980's GE was actively developing an Open Rotor product engine, for installation on the MD-91 & MD-92 applications. The extent of this development program has only recently been acknowledged externally to GE (Majjigi and Wojno, 2011). As shown in Figure 5, the product engine had been designed and was preparing to launch the engine development and certification program, when the program was cancelled in 1989. Although not publicly released until 2011, the GE36 product was designed to achieve nominal compliance with CAEP Chapter 4 requirements (or, alternatively, 10 dB to Chapter 3). As depicted in Figure 6, the product community noise levels were a significant acoustic improvement relative to the aforementioned flight test demonstrators, which was 2dB short of *Chapter 3* compliance, in the 8x8 F7A7 blade configuration, and still had only 2.5 dB nominal margin to *Chapter 3* when tested in the 10x8 configuration.

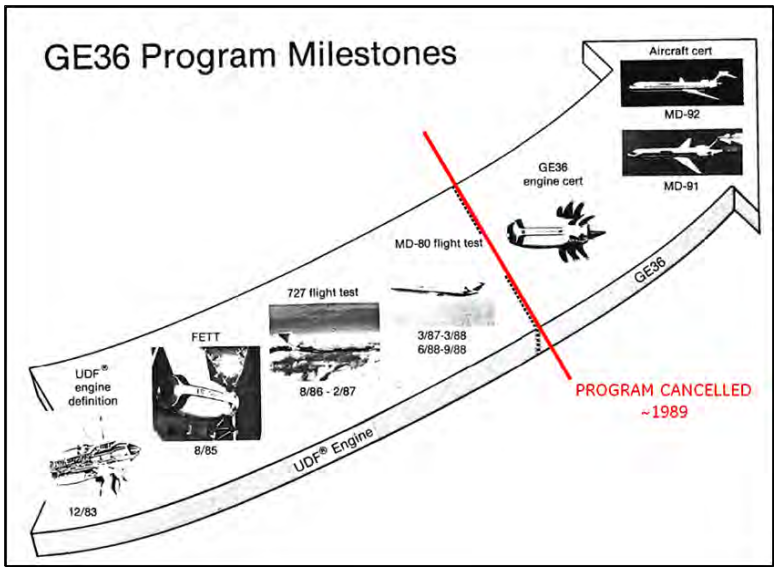

Figure 5: GE 1980's GE36 product development program.

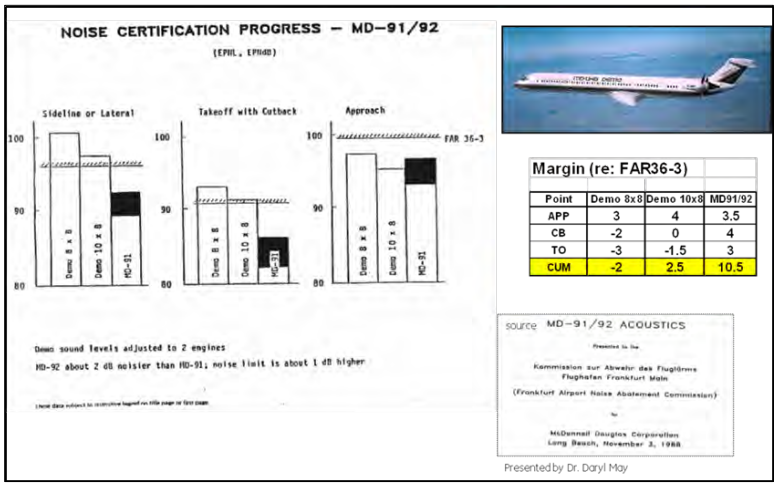

Figure 6: GE36 product acoustic status.

The acoustic improvement of the GE36 product, relative to the UDF® Demonstrator, was achieved by leveraging the noise mitigation strategies identified in Section 1.1. However, modern computational tools were in the infancy, with only limited capability to predict aerodynamic performance, and only empirically based analyses to project noise levels. Consequently, the final product blade designs required a significant trade in aerodynamic performance to achieve the desired community noise levels. The product acoustic blade design, designated F53A53, achieved nominal Chapter 4 compliance, but sacrificed ~3% cruise efficiency, relative to a corresponding aerodynamic performance design, F54A54, which did not include the acoustic mitigation design features. Furthermore, even the latter design contained some aerodynamic compromises, such that it missed the performance levels of the 1980's best aerodynamic blade design (F31A31), by approximately 2%. Thus, the GE36 Product acoustic blade designs achieved nominal Chapter 4 compliance at approximately a 5% penalty in aerodynamic performance relative to the aero performance entitlement design, F31A31. Since the objective of the Modern Open Rotor Aeroacoustic Technology was to provide the maximum fuel burn benefit, relative to the reference engine, CFM56-7B, the 1980's aero performance entitlement design was selected as the

historic design parent for all of the modern open rotor blade concepts. To ensure that the test program captured the acoustic and aerodynamic performance levels relative to the parent, the F31A31 Historic Baseline blades were remanufactured and extensively tested in the Gen1 test campaign of the open rotor technology development program described below.

Section 2.4: Modern Open Rotor Technology Development Program

State-of-the-art computational fluid dynamics (CFD) and computational aero-acoustics (CAA) have enabled progress in open rotor aero-acoustic design beyond what was achieved decades ago. The analytical techniques employed during this research were used to tailor the blade shape for low noise at low flight speed conditions in such a way as to retain much of the efficiency at high flight speed by avoiding shock losses and boundary layer separation.

Testing was conducted in collaboration with NASA Glenn Research Center. The acoustically treated 9x15 Low Speed Wind Tunnel (LSWT) was used to evaluate low flight speed acoustics. The porous walled 8x6 High Speed Wind Tunnel (HSWT) was used to evaluate high flight speed performance.

The technology maturation program encompassed the following segments: Gen1 design, Gen1 low speed testing, Gen2 design, high speed testing, and Gen2 low speed testing. Gen1 design work was carried out under GE independent research and development funding. NASA refurbished the open rotor propulsion rig (ORPR), formerly called the Model Propulsion Simulator (MPS) (Sullivan, 1990), and supplied the test facilities, data acquisition, and support personnel. Under the Continuous Lower Energy, Emissions, and Noise (CLEEN) program, the FAA provided cost-share support for all of the Gen2 testing and design work that was carried out after the first round of low speed testing.

Figure 7 shows the trend of propulsive efficiency, η_{prop}, with fan pressure ratio for 0.80 flight Mach number and 1.0 adiabatic efficiency, η_{adia} (assuming ideal gas with ratio of specific heats of 1.4). Open rotors at cruise have a fan pressure ratio below 1.1 which gives a substantial propulsive efficiency benefit over ducted turbofans for which nacelle weight, drag, and duct losses limit the optimum fan pressure ratio for minimum fuel burn as indicated in Figure 7. The benefits of low fan pressure ratio become more pronounced at lower flight speeds, hence, open rotors provide more significant benefits on short range missions.

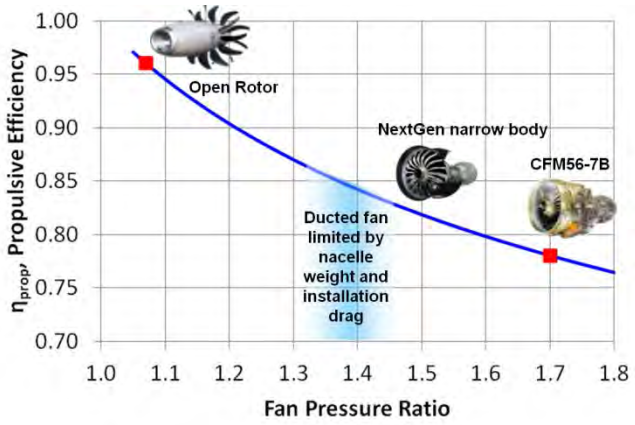

Figure 7: Propulsive efficiency, η_{prop}, trend with fan pressure ratio for 0.80 flight Mach number.

Although propulsive efficiency is important, it does not fully characterize the performance of the propulsion system. Wake and shock losses captured by adiabatic efficiency, η_{adia}, and induced losses resulting from exit swirl and unrecovered kinetic energy associated with wakes and tip vortices must also be taken into account. To encompass all of these effects, overall propeller net efficiency, η_{net}, is used to characterize aerodynamic performance.

The goals of the program were established to achieve a 26% reduction in fuel burn relative to CFM56-7B powered narrow body aircraft while maintaining sufficient noise margin to ensure compliance with anticipated future CAEP Chapter 5 community noise requirements. The acoustic goal was set to 15-17 EPNdB margin relative to Chapter 4 to accommodate a 10 dB margin guarantee with 5-7 dB airframe development execution margin.

Doing a detailed aircraft fuel burn study accounting for the multiple aircraft configurations and engine installation issues was outside the scope of this open rotor technology maturation program. Therefore, the program undertook a simplified fuel burn analysis to capture some of the most significant effects of the propulsion system to arrive at a max climb design point overall net efficiency target.

GE's fuel burn analysis was based on an internal model of a Boeing 737-800W 162 seat aircraft for an 800 nm mission at Mach 0.78 cruise. The model accounted for changes in the weight and drag associated with engine size, but not associated airframe changes or changes in installation effects drag. Also built into the fuel burn analysis are improvements in core engine efficiency projected for a 2025 entry to service. Figure 7 shows that the cruise η_{prop} benefit of open rotor relative to a CFM56-7B is approximately 18%. Not all of this benefit would be realized in fuel burn due to weight and drag penalties as well as noise reduction features, but most of the 26% fuel burn goal is based on the improved η_{prop}. Aircraft improvements, such as in wing aerodynamics and weight reductions due to materials were not incorporated into the analysis.

Table 1 provides the conditions for max climb and takeoff developed for the cycle model used for the fuel burn analysis. For aerodynamic performance, the focus was on max climb where the Mach numbers through the blades are the highest. Thus, although η_{net} was obtained for both points (as well as all other points along the mission), only the 0.860 max climb overall propeller net efficiency was used as the performance target for this program. While the single-point efficiency target derived from the rather crude fuel burn analysis can be argued to be overly simplistic, it is emphasized that the purpose of the program was to bring the technology to a state at which the fuel burn and acoustic goals can be achieved on *future* (yet undefined) aircraft. Thus, throughout the remainder of this paper, the open rotor performance figure of merit is Mach 0.78 max climb η_{net}. Also, because some of the improvement in fuel burn is due to core engine efficiency, propeller η_{net} is used to indicate progress with respect to historical designs.

		Max Climb	*Takeoff*
Altitude	ft	35,000	0
ISA+	°F	18	27
Mach		0.78	0.25
F_{net}	lbf	4,842	24,003
P_{shaft}	hp	7,946	18,509
η_{net}		0.860	0.675

Table 1: Propeller cycle points developed to correspond to a 26% fuel burn reduction relative to CFM56-7B powered aircraft.

As indicated previously, the program acoustic goal was to demonstrate 15-17 EPNdB cumulative margin relative to CAEP Chapter 4, which requires an aircraft specific community noise assessment along a given trajectory. Because the specific operating conditions for a commercial aircraft application are proprietary, the NASA modern open rotor aircraft described in Guynn, et al. (2012) was selected for assessment of acoustic performance relative to the goal. Figure 8 and Table 2 provide the acoustic certification conditions. The initial Gen1 assessment was jointly developed by GE and NASA, under the GE/NASA RTAPS collaboration. The Gen1 results presented below are consistent with the prior NASA publication.

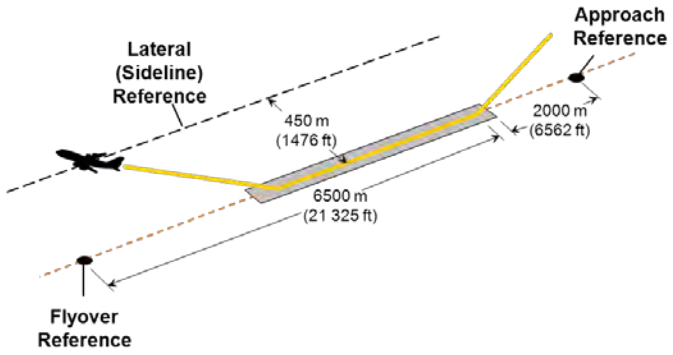

Figure 8: Noise observer arrangement relative to takeoff and landing aircraft trajectories.

		Approach	*Sideline*	*Cutback*
Altitude	ft	389.79	979.21	2038.17
MGTOW	lb	140,796	155,135	151,080
TAS	kts	136.71	177.40	180.23
F_{net}	lbf	11,555	36,170	22,543

Table 2: Acoustic certification conditions for NASA modern open rotor aircraft (both engines).

CHAPTER 3. EXPERIMENTAL SETUP

The rig, instrumentation, and test setup are similar to those described in Sullivan (1990) and the specific model hardware was the SN003 consisting of a forebody, afterbody, rotating hubs for the R1 (forward) and R2 (aft) blade rows, and a selection of spacers.

Rig net thrust, F_{net}, is obtained as described for effective thrust in Sullivan (1990) based on both balance measurements and integrated pressure forces on the rig. Figure 9 is a schematic diagram of the rig without pylon showing the forces used. The rotor hub forces, F_{h1} and F_{h2}, are obtained from the balance measurements corrected by the upstream and downstream rotor hub face pressure area-integrals to get the thrust force on the rotor hub. Nacelle pressure forces, corresponding to rig forebody and afterbody forces, F_{fb} and F_{ab}, are computed as pressure area-integrals with upstream facing projected area treated as positive. The net thrust is change in rotor hub and nacelle forces due to the action of the blades, so it requires knowing the forces with blades installed, as well as without the blades at the same flight conditions. Thus, F_{net} is computed as the difference in the rotor hub forces, blades-on minus blades-off, minus the difference in nacelle pressure forces, blades-on minus blades off, i.e.,

$$F_{net} = (F_{h1} + F_{h2})^{*} - (F_{h1} + F_{h2})^{**} - [(F_{fb} + F_{ab})^{*} - (F_{fb} + F_{ab})^{**}]$$

* Blades-on
** Blades-off

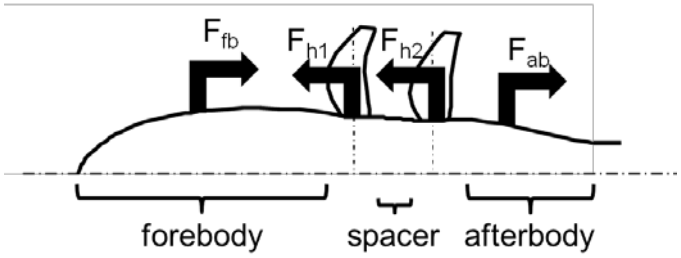

Figure 9: Rig schematic showing forces.

Mach number corrections to account for the blockage presented by the open rotor test rig in the HSWT were obtained in the same manner as described in Stefko and Jeracki (1988). NASA incorporated the Mach number adjustment into the data processing system so that measured Mach number represented the projected flight Mach number rather than the lower value that would be obtained from tunnel total and static measurements.

Figure 10 shows the ORPR installed in the LSWT. This facility features an acoustically treated test section, as shown. The pylon shown was designed and scaled to adequately support an open rotor engine without excessive wake penalty. In addition, trailing edge blowing was built into the pylon design to partially mitigate noise penalties of pylon wake ingestion into the blades during low altitude flight. Angle of attack was achieved by pivoting the rig horizontally at the base of the swept support strut. Acoustic data was collected using a single traversing microphone (not shown), along a 1.52 m (60 in) sideline location, measured relative to the rig at zero angle of attack. During testing, the microphone traveled axially to include observer angles of 18 to 140°, such that 90° corresponded to the R2 pitch change axis station.

Figure 10: ORPR with historical blades installed in the LSWT *(Courtesy NASA)*.

As validation of the approach used in this program to quantify full scale noise from sub-scale rig test data, Figure 11 reproduced from Gliebe (1988) shows a historical comparison of flyover flight test data with corresponding projected levels based on GE's Cell-41 test data for the 1/5th scale MPS rig. Good comparisons were observed, allowing for some confidence in both the evaluation of noise reduction trends as well as projecting expected community noise margins while carrying out our current test program ahead of a potential flight demonstrator in the future.

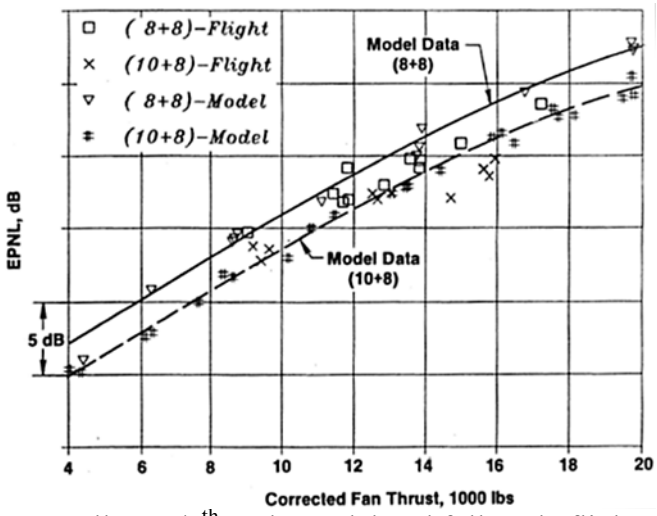

Figure 11: Comparison of GE Cell-41 1/5th scale model and full-scale flight test data. Reproduced from Gliebe (1988).

CHAPTER 4. ANALYSIS METHODOLOGY

Blade design was guided by steady multi-bladerow Reynolds-Averaged Navier-Stokes (RANS) CFD with mixing plane between the two rotors at both max climb and takeoff conditions, paying close attention to flow features relevant to efficiency and acoustics. Boundary conditions were obtained from an axisymmetric streamline curvature calculation in which 20% of the mass flow passes through R1. As described in Smith (1987), the flow properties from the blade tip to outer boundary (including the outer boundary streamline itself) are obtained using the method of Smith and Pierce (1958) and Hess and Smith (1952). The inlet and exit of the CFD domain were placed a few blade chord lengths upstream and downstream of the blade row edges. A 1-D Riemann invariant far-field boundary condition was implemented for the outer boundary, which was conical in shape to avoid numerical artifacts associated with varying inflow/outflow velocities. Loss and radial loading distributions from CFD were then reapplied to the axisymmetric calculation to update the boundary conditions for subsequent CFD calculations.

The Computational Aero-Acoustics (CAA) analysis approach used to guide the low-noise blade design used an in-house prediction capability as presented in Sharma and Chen (2012), which will be described briefly below. First, a steady multi-bladerow mixing plane RANS computation as described above is performed (see Figure 12), iteratively modifying the R1 and R2 pitch angles to target the desired thrust at the acoustic condition of interest (typically takeoff). The R1 wakes are then extracted closely behind the fan trailing edge and a separate RANS-based wake propagation analysis (assumed steady in the R1 reference frame) is performed on a refined mesh to ensure a grid-independent prediction of the wake profiles at the R2 inlet interface. Gust harmonics profiles are then extracted from the wake propagation solution to determine the wake forcing function specified at the R2 inlet for the linearized unsteady RANS analysis for the interaction tone noise response at R1 blade passing harmonics in the R2 relative frame of reference. The unsteady solution is then sampled on an enclosing Ffowcs Williams-Hawkings (FW-H) surface, replicated analytically to provide a full-annulus source field, and propagated to an array of farfield observer locations.

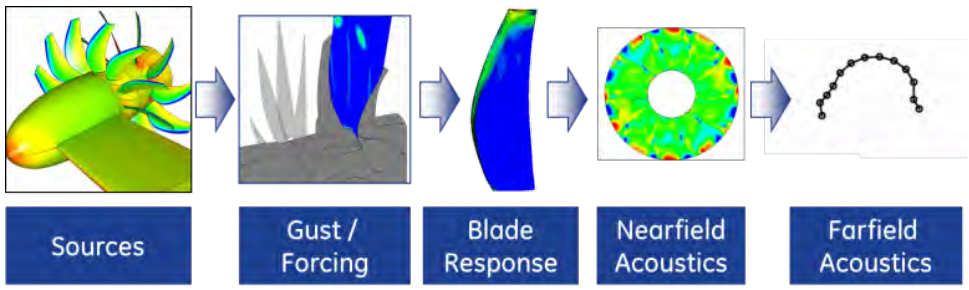

Figure 12: Overview of open rotor noise prediction process.

For a representative baseline configuration, grid refinement level and operating condition, a sensitivity assessment is performed to ascertain an appropriate choice of the FW-H surface such that conclusions drawn while comparing different blade designs appear insensitive – i.e., the surface must be placed far enough from the blade surface to include the majority of quadrupole sources (if necessary), yet not so far that numerical errors have degraded the quality of the source field at the FW-H surface. Finally, the farfield directivity is integrated to determine tone power levels for the various propeller self and interaction tones of interest.

CHAPTER 5. AEROACOUSTIC DESIGN

The designs developed in the present program built on the design trends established during the UDF® program of the 1980's. To ensure consistency with the historical database, one historical design was analyzed and tested along with the modern designs. The historical design selected for this study was a 0.78 cruise Mach number "best-aero" design (called F31A31). Note that this is not an earlier 0.72 cruise Mach number design (called F7A7) actually flown on the UDF® demonstrator aircraft. A comparison of blade design parameters is given in Table 3, followed by discussion of several key design choices.

Parameter		*Historical*	*Modern*
Blade count		12x10	12x10
R1 diameter, *D*	ft	10.7	14.0
Design point disk loading	hp/ft^2	100	59
Spacing/diameter, *S/D*		0.28	0.27

Table 3: Comparison of key parameters for historical and modern designs.

Blade count – Notionally, it is desirable to maximize the blade counts to reduce loading per blade, which reduces induced losses as well as loading and rotor-rotor interaction noise. Note the rotor-rotor interaction noise is affected in two ways: the R1 blade loading directly affects the strength of its shed wakes and vortices, and the R2 blade loading affects its unsteady response to the incoming R1 gusts. These effects must be adequately accounted for in order to properly optimize the blade counts and blade design. Mismatched blade counts between forward and aft rotors, as demonstrated historically in Figure 11, can also significantly affect acoustic radiation efficiencies of the rotor interaction tones. The blade count selection is therefore an important consideration, but is limited however by considerations of the pitch change mechanism, blade solidity for reverse thrust, and engine weight. All configurations in the research presented here used 12 forward and 10 aft blades.

Diameter – The aggressive acoustic target and the strong relationship between disk loading (power per unit propeller annulus area) and noise led to an increase in propeller diameter from roughly 3.25 m (10.7 ft) for 1980's UDF® designs to 4.27 m (14.0 ft) for this research. The increased diameter improves the net efficiency (by 2 to 3%) via increased propulsive efficiency, but also increases the weight and installation penalties which can offset the fuel burn benefit associated with the propulsive efficiency gains. The acoustics benefit for the lower disk loading, however, is quite significant. The historical 1980's design that was fabricated and tested in this program has a max climb design point disk loading of 803 kW/m^2 (100 hp/ft^2) full-scale. For the modern designs, the max climb disk loading is 474 kW/m^2 (59 hp/ft^2).

Aft clipping – As mentioned above, the interaction of the R1 tip vortex on R2 represents an important noise source, particularly at high thrust and low flight speed conditions such as takeoff in which the propeller streamtube contracts more than at the high flight speed design point. The schematic diagram of Figure 13 illustrates two blade rows with a representative design point R1 tip streamline. Clipping is defined as the distance of the R2 tip from this streamline. To guide R2 clipping optimization, two clipping levels were tested: a baseline clipping level (not quantified here) and an additional 5% aft blade span reduction.

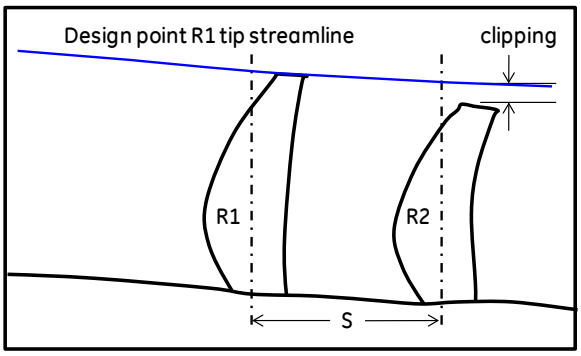

Figure 13: Open rotor tip streamline illustrating aft clipping.

Spacing – The program used the existing MPS rig design from the UDF® program. As described in the experimental setup, this rig used multiple hub spacers to allow the study of the effects of inter-rotor spacing. Generally, increasing spacing reduces noise by mixing the wakes and vortices prior to their impingement on the aft rotors; however, because of the streamtube contraction through the rotors, the impingement location of the R1 tip vortex on R2 migrates inboard as the inter-rotor spacing is increased. Therefore, the R2 clipping level must be adequately optimized while taking into account competing effects of spacing, loading and efficiency. In this research, the largest spacing used on the historical MPS rig was used for all the modern designs and most of the testing. This yielded a spacing to diameter ratio, S/D, of 0.27, where S refers to the distance between rotor pitch change axes (dashed vertical lines in Figure 13). For the historical design, S/D was 0.28 and a significant amount of testing was carried out at 0.31.

Design tip speed/RPM – The availability of a variable blade pitch mechanism allows the designer to optimize the rotation speed for a given thrust and operating condition, within mechanical constraints for the open rotors as well as the power turbine. Decreasing tip speed for the high flight speed aerodynamic design point, for example, results in blades with more camber and higher aerodynamic loading. Also, because the blade chords must be adequate for the highly loaded takeoff condition, the lift coefficients at max climb and cruise tend to be lower than required for the optimum lift to drag ratio (Smith, 1987). Thus, for a given takeoff tip speed, not only does lower design tip speed reduce friction losses, but it brings the design lift coefficients closer to the optimum. These benefits are offset somewhat by the higher induced losses associated with the stronger tip vortices.

Pitch Setting – The pitch settings, or equivalently tip speed as discussed above, of both forward and aft rotors can be used to optimize both performance and acoustics. For example, Metzger and Brown (1984) and Magliozzi (1987) showed that increasing R1 tip speed at low flight speed resulted in quieter operation. Equal R1 and R2 RPM are used for all results shown in this paper, although that does not necessarily give the best result for either acoustics or performance.

The designs were analyzed and tested at a range of pitch settings that were set to achieve a given thrust or power and torque ratio at determined R1 and R2 RPM. Increasing the RPM for a given power or thrust requirement corresponds with decreasing the pitch, i.e., increasing (closing) the blade stagger angle. Thus, rather than describing the pitch setting by the setting angles of the blades at a particular radius, the pitch is described herein as forward rotor tip speed (for the engine at flight conditions) for the required power or thrust at the target torque and speed ratios. This provides a consistent nomenclature to compare pitch settings across different configurations.

Figure 14 shows power vs. forward rotor tip speed or RPM for one of the designs tested at 0.78 tunnel Mach number. Each symbol corresponds to a different pitch setting, hence tip speed, required to reach the design power and torque ratio. The scaled design power indicated as the horizontal dashed line corresponds to the full scale max climb P_{shaft} given in Table 1.

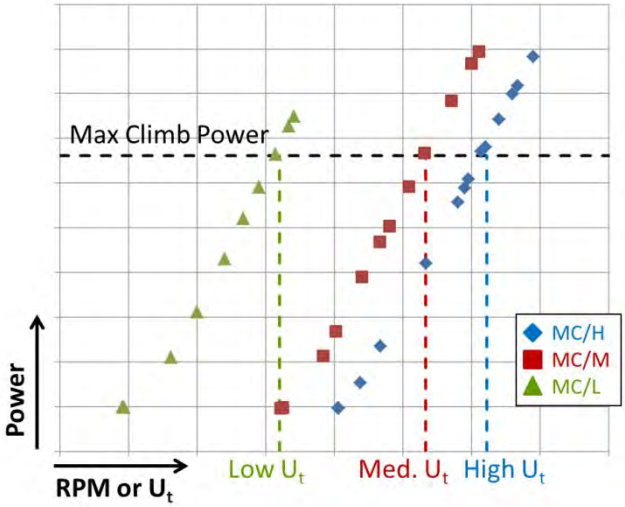

Figure 14: Test data power vs. rotational speed at 0.78 tunnel Mach number indicating the use of tip speed for max climb power to designate pitch settings MC/L, MC/M, and MC/H.

The intersection of each power curve with the desired power defines the rotational speed for the corresponding pitch setting. These pitch settings are henceforth named for the operating condition on which they are based (MC for max climb, TO for takeoff) and a letter indicating low, medium, or high tip speed – e.g., MC/L, MC/M, and MC/H.

A similar approach is used to describe pitch settings for the low speed tunnel testing. For acoustics, the key operating points were takeoff, cutback, and approach. Figure 15 shows thrust vs. tip speed for one of the designs tested at 0.20 tunnel Mach number. Because of tunnel constraints, the low speed testing was performed at a lower Mach number than the desired takeoff Mach number of 0.25. Takeoff thrust, scaled for geometry, tunnel pressure, as well as Mach number to preserve aerodynamic similarity is indicated by the horizontal dashed line.

Three candidate pitch settings for takeoff are designated TO/L, TO/M, and TO/H, for low, medium, and high tip speed, respectively. The "low", "medium", and "high" descriptions refer to the forward rotor. A higher tip speed pitch setting, AP, was designated for evaluation at the approach flight condition.

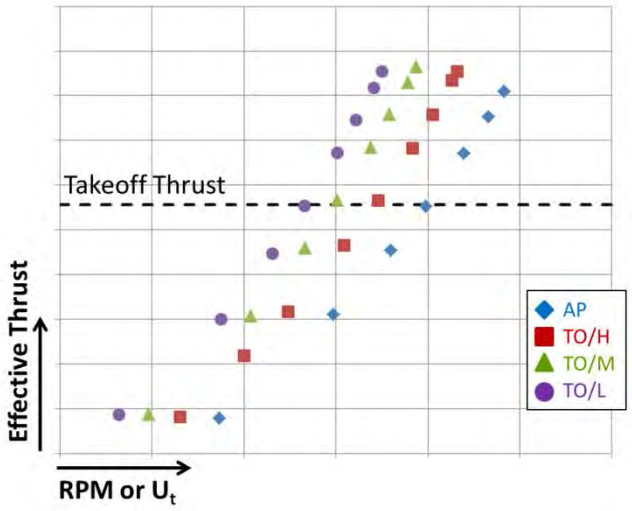

Figure 15: Test data thrust vs. rotational speed at 0.20 tunnel Mach number indicating the use of tip speed for the prescribed cycle point to designate pitch settings.

Blade designs – Several configurations of blade shapes were developed using the analysis methodologies described above. Deformation analysis and fabrication were performed in a similar manner to those described in Sullivan (1990). Proprietary stability criteria were used to assess flutter risk and blade designs were adjusted accordingly to keep the risk low. The blade designs reported in this paper can be summarized as follows:

Historical – One of the first 1980's designs to use CFD (an inviscid Euler-based method). It was demonstrated in the 1980's to have high aerodynamic performance, but did not have features/compromises for acoustics. These are the blades described in Sharma and Chen (2012), Elliott (2011) and Van Zante, et al. (2011) and the design is not the same as that used for the UDF® demonstrator flight program.

Gen1A – Designed for lower disk loading (larger diameter) than Historical and incorporated blade design features to improve takeoff acoustics, particularly controlling the R1 leading edge and tip vortex, while substantially retaining cruise and max climb performance. These features to reduce interaction noise associated with the R1 leading edge and tip vorticity interaction with R2 were incorporated in the subsequent designs as well.

To prevent roll up of the leading edge vortex at high incidence conditions such as takeoff, Gen1A and the other modern designs described below incorporate additional camber near the leading edge so the flow over the suction side of the leading edge remains attached. To enhance tolerance to the resulting negative incidence at high flight speed, two changes to the thickness distribution are incorporated relative to the aero-only design. First, the location of maximum thickness is moved closer to the leading edge. Second, blade thickness is added to the pressure side near the leading edge.

Gen1C – An alternative design to Gen1A to evaluate and better understand the design trades and validate the aero-acoustic prediction methodology in capturing design trends.

Gen1A+B – Design modification to Gen1A intended to specifically reduce interaction noise at takeoff and landing without significant performance penalty at high flight speed.

Gen2A – Redesign in which parameters such as design tip speed, loading distribution, and torque ratio were modified based on lessons learned from the first phase of low speed acoustic testing and additional analytical studies. Torque ratio and tip speed were set to accommodate a geared drive architecture. Compared to Gen1A and Gen1C, Gen2A was designed to reduce the R1-R2 interaction noise contribution of the R1 tip vortex relative to its wake. Also, the 5% additional clipping examined during low speed testing of the Gen1 designs was incorporated into Gen2A. The "+B" features that distinguished Gen1A+B from Gen1A were omitted from this design so as not to confound the effects of the design changes that distinguished Gen2A from Gen1A.

A depiction of the improved acoustics of Gen2A over Gen1A is illustrated in Figure 16, which compares unsteady pressure response on the R2 suction surface due to the 1st harmonic of the R1 wakes at takeoff condition. Shown are 2 dB contour intervals of acoustic pressure level for (a) Gen1A (at the 5% additional clipping level) and (b) Gen2A. Not only is the unsteady pressure for Gen2A substantially reduced, but its special tip profile successfully eliminates the local high level of unsteady pressure caused by the oscillations of its own tip vortex in response to the incoming R1 wakes.

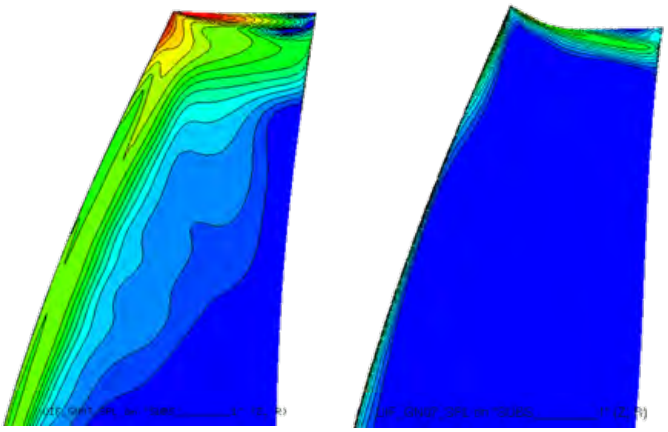

(a) (b)

Figure 16: R2 suction surface unsteady pressure (plotted $20 \cdot \log_{10}|p'|$ with 2 dB contour intervals) due to the 1st harmonic of the R1 wakes for (a) Gen1A with 5% additional clipping and (b) Gen2A.

Gen2A+B – Due to programmatic schedule constraints, this configuration was neither designed nor tested. However, the performance and acoustics status of an open rotor engine based on a Gen2A+B design, constructed by analytically applying to Gen2A the effects of Gen1A+B relative to Gen1A, is presented below. With the reduced R1 tip vortex interaction noise contribution (relative to wake) incorporated in Gen2A, the "+B" technology is anticipated to be at least as beneficial as demonstrated on Gen1A.

CHAPTER 6. RESULTS

The results are organized in the following parts: (A) *tip vortex control,* illustrating the benefits of the R1 acoustic features incorporated into all the designs developed in this program; (B) *acoustic trends and validation,* providing acoustic predictions and experimental trends; (C) *performance,* presenting HSWT rig scale net efficiency; and (D) *final projections,* a summary of the performance and acoustic status at engine scale.

(A) Tip vortex control. As mentioned above, features to reduce the noise associated with the R1 tip vortex interacting with R2 were incorporated into Gen1A and all subsequent designs. Figure 17 shows the results of CFD with relative streamlines through the tip vortex region as well as entropy contours in an axial station downstream for two R1 designs at the takeoff condition: (a) an "aero-only" design for max climb efficiency alone and (b) Gen1A "aero-acoustic" design for low noise as well as high efficiency. For the aero-only design of Figure 17(a), high incidence at takeoff results in leading edge separation in which a leading edge vortex forms and merges with the tip vortex. For the aero-acoustic Gen1A in Figure 17(b), the flow around the leading edge remains attached. The resulting tip vortex defect is smaller than for the aero-only design, so the interaction noise contribution is less for a given R2 clipping (or allows for less clipping for a given acoustic goal). CFD indicates that the max climb net efficiency penalty for the aero-acoustic design feature is less than 0.5%.

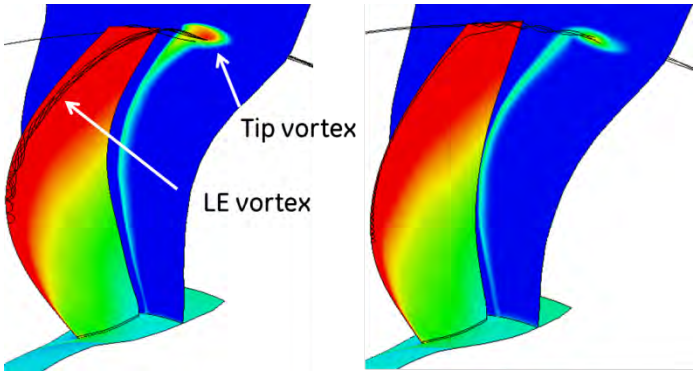

(a) (b)

Figure 17: R1 takeoff condition CFD results for (a) aero-only design and (b) Gen1A aero-acoustic design**.**

(B) Acoustic trends and validation. Figure 18 shows key blade design trends from acoustic predictions as well as experimentally measured data. For each case, the tone power levels from all R1-R2 interaction tones associated with the 1st blade passing frequency of R1 (i.e., 1F+kA for all integers k, where F and A are the blade passing frequencies of the R1 and R2 blades in a stationary frame of reference, respectively) are summed to provide a measure of all the radiated sound power associated with the fundamental gust harmonic of the R1 wakes. Similar comparisons may be made by including higher harmonics of the R1 wakes, to a point where either the numerical model becomes inaccurate and/or the actual spectra from open rotors become more dominated by broadband noise. However, design trends from the low order harmonics of the R1 wakes provide effective guidance for low-noise design.

Absolute tone power levels include uncertainties in both the numerical modeling and test data. Therefore, to more clearly present the ability of the predictions to capture the trend, each graph was plotted by subtracting a constant power level from the predictions such that the points on the left side coincide.

Figure 18(a) shows the acoustic effect of the reduced disk loading and addition of acoustic features for the Gen1A (baseline clipping) with respect to Historical. The prediction captures the experimentally determined trend to within approximately 0.5dB.

Figure 18(b) shows the acoustic trend from Gen1A to Gen1C. The acoustic trend for this design change was successfully captured, as shown, and was used to successfully guide the design of Gen2A.

Figure 18(c) shows the trend for additional 5% R2 clipping from the baseline clipping level for Gen1A. The trend was correctly predicted qualitatively, although the benefit of the additional clipping was over-predicted by approximately 1dB.

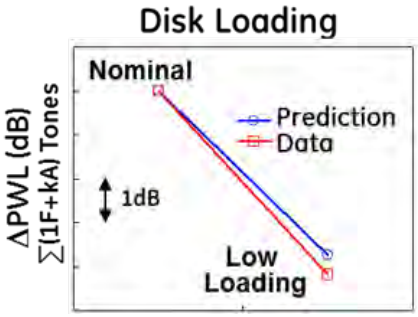

(a)

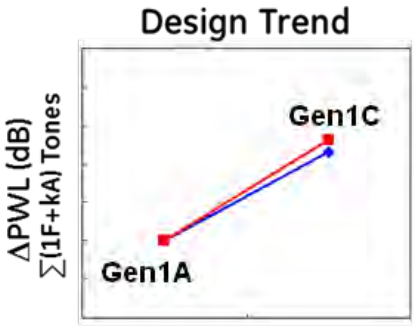

(b)

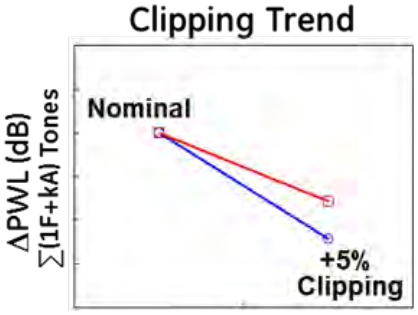

(c)

Figure 18: Acoustic predictions compared to corresponding measured levels for the total sound power level associated with the 1st R1 harmonic interaction tones. *Tick marks represent 1 dB differences.*

(C) Performance. Performance comparisons based on HSWT test data for the different designs and sensitivities to specific features are presented in terms of overall net efficiency, η_{net}. The results are for the isolated nacelle and blades and do not include pylon or aircraft influences. The operating condition is indicated by the tunnel Mach number and a power loading parameter, PQA/J^3, i.e., $P_{shaft} / (\rho_0 V_0^3 A)$.

Figure 19 shows the Mach 0.78 performance for Historical at two pitch settings, MC/L and MC/M. The design PQA/J^3 of 0.167 is shown as the vertical dashed line. At the design power, the tip speed has little effect. As the disk loading decreases, however, the lower tip speed pitch shows more of an advantage.

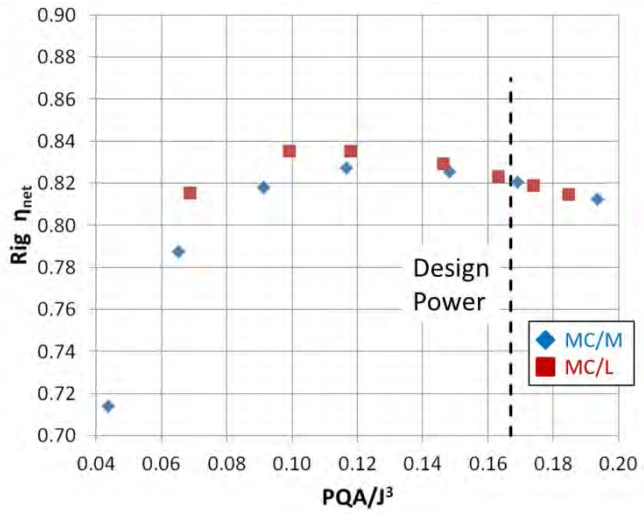

Figure 19: Mach 0.78 net efficiency vs. power loading parameter for Historical design for MC/L and MC/M pitch.

Figure 20 shows Mach 0.78 net efficiency for Gen1A+B at the three pitch settings indicated in Figure 14. This lower disk loading design shows a substantial efficiency benefit for the lower tip speed, with a 2.7% improvement from the highest to the lowest tip speed.

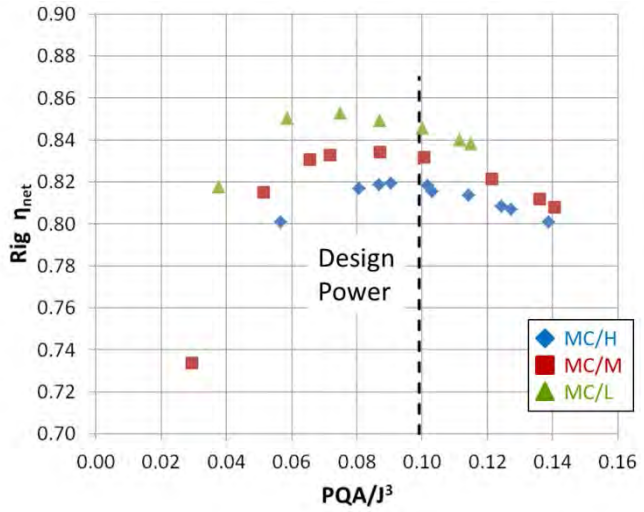

Figure 20: Mach 0.78 net efficiency vs. power loading parameter for Gen1A+B for range of pitch settings.

Although primarily for acoustics, the lower disk loading of the current designs relative to Historical offered an opportunity to improve performance at the aerodynamic design point. Figure 21 shows net efficiency for Historical and Gen1A+B designs (baseline clipping), each at two pitch settings. The design point PQA/J^3 for Historical, 0.167, and modern designs, 0.099, are indicated by the two vertical dashed lines and correspond to the two full scale disk loadings provided in Table 3. Gen1A+B was not tested at the higher disk loading and, as can be seen by the decrease in efficiency as PQA/J^3 increases above its

design value, was not designed for such a high loading. At their respective design disk loadings, Gen1A+B is 1.2 to 2.5% higher in efficiency than Historical, depending on the pitch setting.

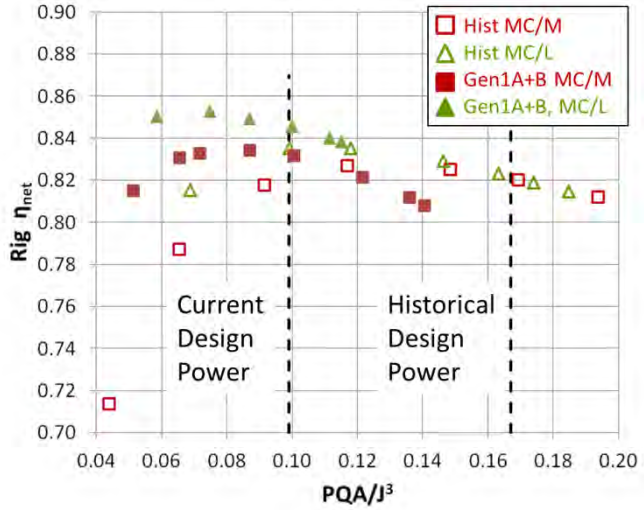

Figure 21: Mach 0.78 net efficiency vs. power loading parameter for Historical and Gen1A+B with baseline clipping, showing two pitch settings for each design.

R2 clipping improves acoustics, but is inherently undesirable for performance because it leaves R1 swirl downstream of the propeller and this wasted kinetic energy reduces the net efficiency. As such, it is important to obtain the performance derivative for clipping.

Figure 22 shows Mach 0.78 net efficiency for Gen1A+B for two clipping levels at MC/M pitch. The additional 5% of clipping from the baseline penalized the net efficiency by 1.2% at the design point.

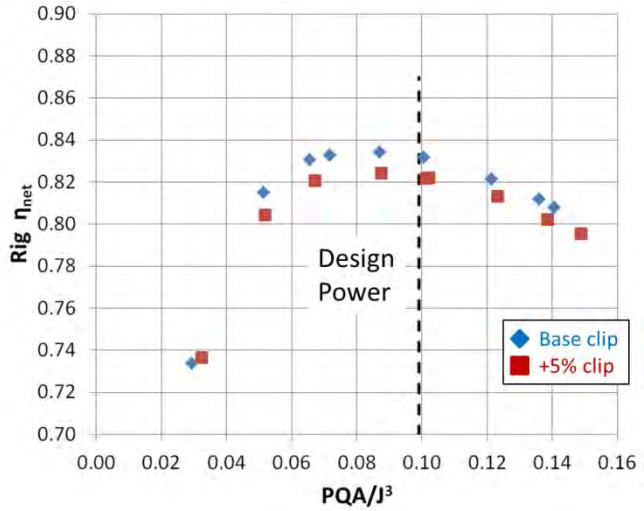

Figure 22: Mach 0.78 net efficiency vs. power loading parameter for Gen1A+B for MC/M pitch for two clipping levels.

Sullivan (1990) found that for pitch axis to pitch axis inter-rotor spacing to diameter ratios, *S*/*D*, of 0.14 to 0.24, the effect on aerodynamic performance was significant, with a 3 to 3.5% increase in net efficiency (at Mach 0.80) as the spacing was decreased. Because of the benefit to acoustics for larger spacing due to increased wake mixing, the current program examined larger spacing to diameter ratios.

Figure 23 shows Mach 0.78 net efficiency for Historical design at MC/L pitch for *S*/*D* of 0.28 and 0.31. The effect of spacing on net efficiency is negligible over this range of inter-rotor spacing.

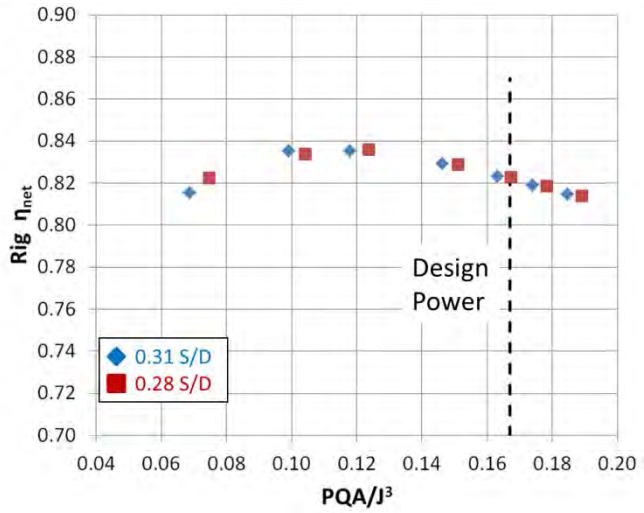

Figure 23: Mach 0.78 net efficiency vs. power loading parameter for Historical for MC/L pitch for two spacings.

In the HSWT, a vibration mode for Gen1A was higher in amplitude than for the other designs. It was not clear that this represented an undue risk to the blades, but it was considered prudent to avoid the highest power settings to ensure that the blades would remain undamaged for subsequent repeat testing in the LSWT Gen2 test campaign. Therefore, to evaluate the performance effect of the "+B" technology below, Gen1A+B is compared with Gen1A at Mach 0.73 rather than Mach 0.78.

Figure 24 shows Mach 0.73 net efficiency for Gen1A and Gen1A+B for MC/M pitch and both clipping levels. At the medium tip speed pitch, the "+B" technology shows 0.5 to 1% efficiency penalty near the peak efficiency range of operation.

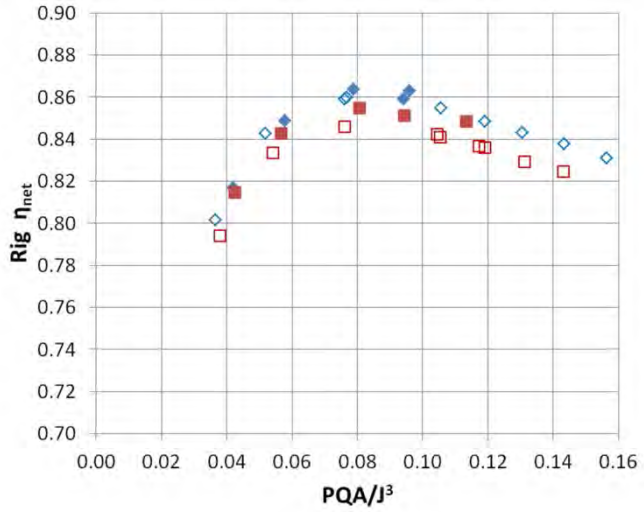

Figure 24: Mach 0.73 net efficiency vs. power loading parameter for Gen1A and Gen1A+B for MC/M pitch and two clipping levels.

Figure 25 shows Mach 0.73 net efficiency for Gen1A and Gen1A+B for MC/L pitch (baseline clipping only). For the lower tip speed pitch setting, the "+B" technology has a negligible effect on performance.

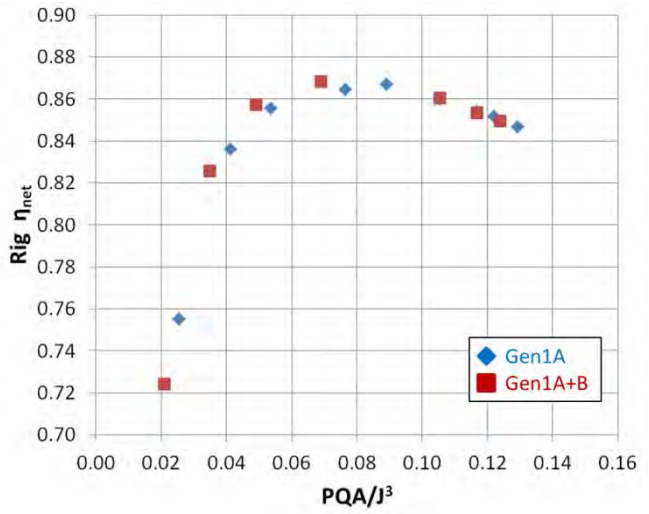

Figure 25: Mach 0.73 net efficiency vs. power loading parameter for Gen1A and Gen1A+B for MC/L pitch.

Figure 20 showed the performance benefit of operating at a low tip speed at design power. Figure 26 shows Mach 0.78 net efficiency for Gen1A+B (all three pitch settings) and Gen2A for its design pitch of MC/L. The trend of the Gen2A data is highlighted with a dashed curve. As with Gen1A, a blade vibration concern in the HSWT led to the decision to refrain from testing the highest power settings. However, sufficient data were obtained to project Gen2A performance to the design point. Using a linear regression fit of the powered points (i.e., omitting windmill) for TQA vs. *J* and PQA vs. *J*, the projected design point performance is indicated by the hollow purple circle shown at the high end of the dashed trend curve. This technique was validated using Gen1A+B data by omitting comparable power points. The extrapolation of the Gen1A+B design point net efficiency was within 0.001 (0.1%) of the measured value. Even with 5% more clipping, Gen2A design point net efficiency is 0.2% higher than that of Gen1A+B.

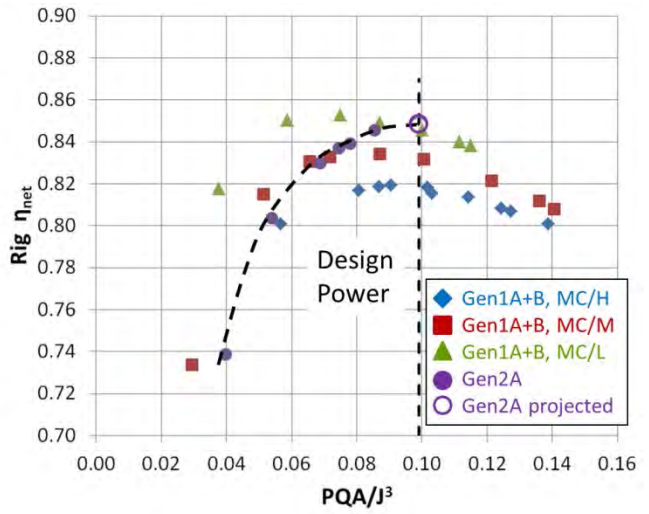

Figure 26: Mach 0.78 net efficiency vs. power loading parameter for Gen1A+B for range of pitch settings and Gen2A at design pitch (MC/L).

(D) Full scale projected status. The results thus far have been presented at rig scale and conditions. However, as stated previously, the program goals were defined in terms of aircraft system levels: -26% fuel burn relative to CFM56-7B and 15-17 EPNdB cumulative margin relative to CAEP Chapter 4. To assess the open rotor technology relative to these goals, full scale projections were generated based on the measured aerodynamic performance from the high speed test campaign and the measured acoustics from the low speed campaign.

Cumulative noise margin to Chapter 4 was evaluated from open rotor measured data scaled analytically to a 4.27 m (14.0 ft) diameter full-scale engine on a model narrow body aircraft as presented in Guynn, et al. (2012). Both the Gen1A+B and Gen2A+B system noise estimates include installation effects, based on the measured generic pusher pylon penalty, partially mitigated by trailing edge wake blowing from the pylon at takeoff and landing. Acoustic measurements taken at multiple angles of attack (0, 3, 8 and 12°) were interpolated to expected rotor inflow angles of attack for the NASA modern open rotor aircraft to assess the corresponding noise penalties.

The overall propeller net efficiency adjustment for full scale Reynolds number at altitude is +0.008 (+0.8%). Figure 27 shows the historical to present progression of full scale propeller (a) altitude max climb overall propeller net efficiency and (b) cumulative community noise margin to Chapter 4. The first bar (red) in each bar graph represents the Historical (aero-only) design from the UDF® program that was tested in the current program. The second bar (purple) represents the acoustic blade design for the GE36 product engine that was developed at the end of the UDF® program and was projected to nominally just meet CAEP Chapter 4 requirements in Majjigi and Wojno (2011). The third bar (blue) is for the Gen1A+B with the 5% additional clipping. The fourth bar (green) is the Gen2A+B, the projected result for Gen2A (designed with the 5% additional clipping) with the additional effects that were determined for the "+B" technology.

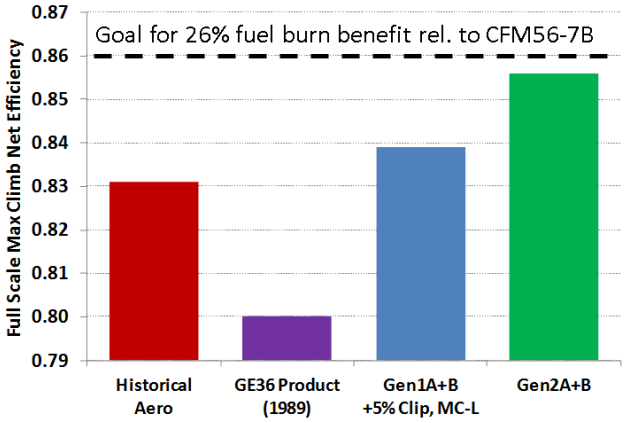

(a)

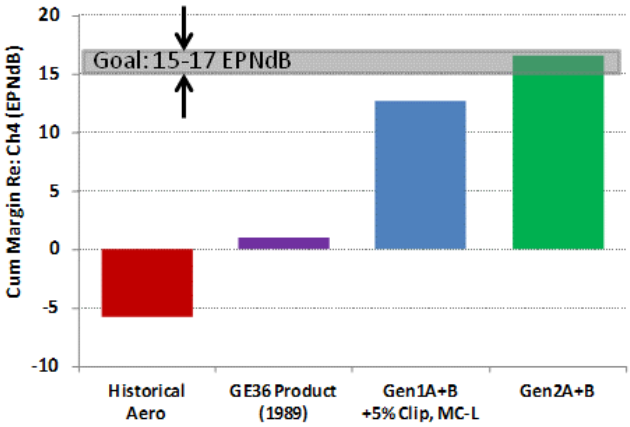

(b)

Figure 27: Progression of projected full scale (a) max climb overall propeller net efficiency and (b) cumulative noise margin to Chapter 4.

For the two historical designs, there was a significant tradeoff between efficiency and noise, with the aero-only design having negative noise margin and the acoustic design suffering in efficiency. This illustrates the dilemma for open rotors by the end of the 1980's.

The Gen1A+B and Gen2A+B results shown do not represent optimized pitch settings from the standpoint of either performance or acoustics. Rather, each bar on the graph represents a reasonable pitch angle (or tip speed) choice in light of the completeness of the data acquired. For max climb efficiency the MC/L pitch setting was used. However, time constraints did not allow for exploration of the pitch angle space to find the optimum. For community noise estimates, the TO/M pitch setting was used, although testing identified other pitch settings that yielded lower noise for certain trajectory points. The conservatism built into the selection of pitch settings used for the projected status leaves room for further improvements that may be required as the aircraft configuration and certification issues become more defined.

The Gen1A+B max climb net efficiency shown in Figure 27(a) is obtained from MC/L pitch test data with baseline clipping with an additional 1.4% penalty applied for 5% additional clipping. The clipping penalty of 1.2% determined at the MC/M pitch was increased by 20% to account for the increased swirl associated with lower tip speed. However, the acoustic result for this Gen1A+B with the 5% additional clipping is based on direct measurements for this configuration. This design, with lower disk loading and acoustic blade design features, achieves significantly improved high flight speed performance as well as

low flight speed acoustics compared to either of the historical designs. The Gen2A+B design further improves upon both max climb efficiency and acoustic margin. As shown in Figure 25, the "+B" technology had negligible effect on performance at the MC/L pitch. However, because of the proprietary nature of that noise reduction technology, its contribution to the noise margin is not presented here.

The noise results indicate that substantial benefits were obtained in the modern test campaign beyond what would be achievable by disk loading benefits alone, i.e., by simply increasing the fan diameter for a given thrust. Furthermore, in addition to pitch optimization mentioned above, pylon trailing edge blowing can be optimized further than what was initially performed here on the sample generic pylon design. It is also possible that incorporating into the Gen2A design the "+B" technology, rather than analytically applying its effects as described above, would yield better performance and acoustics than what is currently presented in Figure 27.

As in the results presented here, Guynn, et al. (2012) also showed a substantial benefit of open rotor compared to current technology turbofans. Using data obtained for Gen1A+B with 5% additional clipping, the NASA study projected a 36% improvement in block fuel burn relative to a 1990's technology aircraft. The fuel burn analysis was more sophisticated than that used in this program and involved additional aircraft technologies and a different mission. However, the results provide an independent validation that the η_{net} target established in this program does indeed correspond to fuel burn benefits in line with the program goal. In addition, using the same low flight speed trajectory as used in this program, Guynn, et al. (2012) obtained 12.6 EPNdB noise margin to Chapter 4, nearly the same as shown in Figure 27(b).

Because propellers are typically restricted to lower flight speeds than turbofans, it might be assumed the cruise Mach number for open rotor should be lower as well. However, the test results show that such a restriction is unnecessary. Figure 28 shows Gen1A+B (baseline clipping) full scale overall propeller net efficiency as a function of flight Mach number. The cruise thrust conditions were obtained from the cycle model developed for the current open rotor technology development program. Also, the pitch setting is MC/L throughout, not optimized for each condition. The data shows that the net efficiency remains above 0.85 over the Mach number range up to 0.80. For this reason, the cruise and max climb Mach number of 0.78 is reasonable for open rotor aircraft.

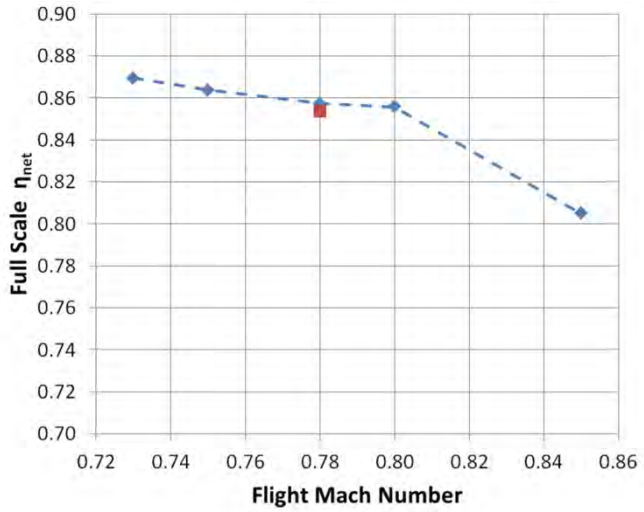

Figure 28: Full scale Gen1A+B cruise net efficiency trend at MC/L pitch and max climb design point efficiency (square) as a function of test flight Mach number.

CHAPTER 7. CONCLUSIONS

In partnership with NASA and the FAA, the five-year, two-phase open rotor technology development program has demonstrated the aggressive performance and acoustic goals established at the beginning of the technology development program. The goals were derived from the anticipated fuel burn and noise requirements of future narrow body aircraft. CAA tools captured the trends of disk loading, design changes, and clipping and were useful to provide guidance for low noise designs. In addition to providing input to guide the Gen2 design, the Historical and Gen1 testing explored the effects of disk loading, clipping, and inter-rotor spacing.

The performance effects of design features relevant for noise were assessed. The examined blade pitch setting, equivalently expressed as tip speed to achieve the design power and torque ratio, had a substantial effect on Gen1A+B max climb performance, with a 2.7% improvement in net efficiency from the highest to the lowest tip speed. However, the Historical blades at their design point were insensitive to a similar range of pitch settings. An additional 5% span aft blade clipping resulted in approximately 1% reduction in max climb net efficiency. Spacing to diameter changes from 0.28 to 0.31 had a negligible effect on efficiency. The noise mitigation technology "+B" was found to have a negligible effect on performance when tested at the low tip speed pitch setting that was selected as the design point tip speed for Gen2A.

Unlike designs of the 1980's in which the blades were only marginally satisfactory for either high flight speed performance or low flight speed acoustics, modern analytical tools have enabled current designs to meet aggressive acoustic goals while retaining the performance advantage of low disk loading, even at flight Mach number up to 0.80.

The Gen2A+B results were analytically constructed by combining direct measured results of Gen2A with the measured effects of technology "+B" with respect to the tested Gen1A baseline design. A Gen2A+B design is projected to meet the noise goal of 15-17 EPNdB cumulative margin to Chapter 4 on the NASA modern open rotor aircraft model while coming within 0.5% of the Mach 0.78 max climb net efficiency goal for 26% fuel burn benefit relative to CFM56-7B powered aircraft. These projections do not include additional improvement opportunities demonstrated during the test campaign with regard to pitch setting, pylon blowing, and blade design that can be employed to further advance open rotor technology.

CHAPTER 8. EMISSIONS

While the topic of engine emissions was not specifically investigated as part of the open rotor technology development program, the advances in aerodynamic performance that were demonstrated experimentally translate into improvements in emissions as well. For the mission studied, because it is projected to have a 26% reduction in fuel burn relative to the baseline engine, a low-noise open rotor engine offers a 26% reduction in overall exhaust emissions due to reduced fuel burn alone. In addition, further advancements for such an engine, such as demonstrated with the TAPS-II combustor under its own CLEEN program, are anticipated to bring further reductions in unburned hydrocarbons, NOx, and CO.

CHAPTER 9. ACKNOWLEDGEMENTS

In addition to thanking GE for permission to publish these results, the authors wish to thank NASA and the FAA for their partnership in developing open rotor technology. NASA Glenn Research Center personnel led by Dale Van Zante worked tirelessly to ensure that the test program was successful. Also, partnership with NASA under the Environmentally Responsible Aviation (ERA) program facilitated full scale noise assessments presented here. The keen interest, valuable feedback, and sponsorship of the FAA, led by contract monitor Rhett Jefferies, was critical to the success of the program. Significant funding came from the FAA under a Continuous Lower Energy, Emissions, and Noise (CLEEN) contract. A debt of gratitude further extends to numerous individuals at GE who provided support for analysis and design, hardware fabrication and testing of the configurations described in this paper. The results presented in this paper are possible only because of their expertise and significant contributions to the program.

CHAPTER 10. NOMENCLATURE

A	forward rotor annular area
D	forward rotor diameter
EPNL	effective perceived noise level
F_{ab}	afterbody pressure force
F_{fb}	forebody pressure force
F_{h1}, F_{h2}	forward and aft rotor hub forces, respectively
F_{net}	propeller net thrust
ISA	International Standard Atmosphere
J	forward rotor advance ratio, $V_0 / (N D)$
kA	k^{th} blade passing frequency of R2
MGTOW	maximum gross takeoff weight
N	angular speed, rev/s
nF	n^{th} blade passing frequency of R1
P_{shaft}	shaft power for both rotors combined
p'	unsteady pressure
PQA	power coefficient, $P_{shaft} / (\rho_0 N^3 D^3 A)$
R1, R2	forward and aft blade row, respectively
S	R1 and R2 pitch change axes axial spacing
TAS	true airspeed
TQA	thrust coefficient, $F_{net} / (\rho_0 N^2 D^2 A)$
U_t	forward rotor tip speed
V_0	flight or tunnel freestream velocity
V_e	exhaust velocity expanded to ambient
W_a	actual work input for stagnation pressure rise
W_s	work input assuming isentropic process
η_{adia}	adiabatic efficiency, W_s / W_a
η_{net}	overall net efficiency, $F_{net} V_0 / P_{shaft}$
η_{prop}	propulsive efficiency, $2 V_0 / (V_0 + V_e)$
ρ_0	freestream air density

CHAPTER 11. REFERENCES

Elliott, D. M., "Initial Investigation of the Acoustics of a Counter Rotating Open Rotor Model with Historic Baseline Blades in a Low Speed Wind Tunnel," AIAA 2011-2760, 17th AIAA/CEAS Aeroacoustics Conference, Portland , OR, June 2011.

Gliebe, P. R., "Flight Test vs. Model Test UDF® Engine Noise," Royal Aeronautical Society Conference, Advanced Propellers and their Installation on Aircraft, Cranfield Institute of Technology, England, Sept. 26-27, 1988.

Guynn, M. D., Berton, J. J., Haller, W. J., Hendricks, E. S., and Tong, M. T., "Performance and Environmental Assessment of an Advanced Aircraft with Open Rotor Propulsion," NASA/TM-2012-217772, NASA Langley Research Center, Hampton, VA, 2012.

Harris, R. W. and Cuthbertson, R. D., "UDF™ /B727 Program," AIAA 1987-1733, AIAA/SAE/ASME/ASEE 23rd Joint Propulsion Conference, San Diego, CA, June-July 1987.

Hess, J. L. and Smith, A. M. O., "Calculation of Non-lifting Potential Flow About Arbitrary Three Dimensional Bodies," Douglas Aircraft, Report No. ES 40622, 1962.

Hoff, G. E., "Experimental Performance and Acoustic Investigation of Modern Counter-rotating Blade Concepts," NASA CR-185138, January 1990.

Magliozzi, B., "Noise Characteristics of a Model Counterrotating Prop-Fan," 11th AIAA Aeroacoustics Conference, AIAA-87-2656, Sunnyvale, CA, 1987.

Majjigi, R. K. and Wojno, J. P., "Previous Open Rotor Experience at GE and Source Noise," EU X-Noise Open Rotor Technology Seminar, Lausanne, Switzerland, March 2011.

Metzger, F. B. and Brown, P. C., "Results of Acoustic Tests of a Prop-Fan Model," AIAA/SAE/ASME/ASEE 23rd Joint Propulsion Conference, AIAA-87-1894, San Diego, CA, 1984.

Nichols, H. E., "UDF™ Engine/MD-80 Program," AIAA 1988-2805, AIAA/SAE/ASME/ASEE 24th Joint Propulsion Conference, Boston, MA, July 1988.

Podboy, G. G. and Krupar, M. J., "Laser Velocimeter Measurements of the Flowfields Generated by an Advanced Counter-rotating Propeller," AIAA 1989-0434, 27th Aerospace Sciences Meeting, Reno, NV, January 1989.

Ravindranath, A. and Lakshminarayana, B., "Mean Velocity and Decay Characteristics of the Near and Far Wake of a Compressor Rotor Blade of Moderate Loading," Journal of Engineering for Power, Vo. 102, No. 3, July 1980.

Sharma, A. and Chen, H., "Prediction of Tonal Aerodynamic Noise from Open Rotors," 18th AIAA/CEAS Aeroacoustics Conference, AIAA-2012-2265, Colorado Springs, CO, 2012.

Shin, H. W., Whitfield, C. E., and Wisler, D. C., "Rotor-Rotor Interaction for Counter-Rotating Fans; Three-Dimensional Flowfield Measurements," *AIAA Journal*, Vol. 32, No. 11, November 1994.

Shivashankara, B. N., Johnson, D. P., and Cuthbertson, R. D., "Installation Effects on Counter Rotating Propeller Noise," AIAA 1990-4023, 13th Aeroacoustics Conference, Tallahassee, FL, October 1990.

Smith, A. M. O. and Pierce, J., "Exact Solution of the Neumann Problem, Calculation of Non-circulatory Plane and Axially Symmetric Flows About or Within Arbitrary Boundaries," Douglas Aircraft , Report No. ES 26988, 1958.

Smith, L. H., "Unducted Fan Aerodynamic Design," ASME Journal of Turbomachinery, vol. 109, pp. 313-324, 1987.

Stefko, G. L. and Jeracki, R. J., "Porous Wind Tunnel Corrections for Counterrotation Propeller Testing," NASA/TM-100873, 1988.

Sullivan, T. J., "Aerodynamic Performance of a Scale-Model, Counterrotating Unducted Fan," ASME Journal of Turbomachinery, vol. 112, pp. 579-586, 1990.

Van Zante, D. E., Gazzaniga, J. A., Elliott, D. M., and Woodward, R. P., "An Open Rotor Test Case: F31A31 Historical Baseline Blade Set," ISABE 2011-1310, International Society of Air Breathing Engines, Gothenburg, Sweden, Sept 2011.

CHAPTER 12. ADDITIONAL REFERENCES

Delaney, B. R., Balan, C., West, H., Humenik, F.M. and Craig, G., "A Model Propulsion Simulator for Evaluating Counter-rotating Blade Characteristics," Paper 861715, Society of Automotive Engines, Aerospace Technology Conference, Long Beach, CA, Oct. 1986.

Janardan, B. A. and Gliebe, P. R., "Acoustic Characteristics of Counter-rotating Unducted Fans from Model Scale Tests," *Journal of Aircraft*, Vol. 27, No. 3, March 1990.

Majjigi, R. K. and Gliebe, P. R., "Development of a Rotor Wake/Vortex Model," NASA CR-174849, June 1984.

Hughes, C. E., "Flowfield Measurements in the NASA Lewis Research Center 9-by 15-foot Low-Speed Wind Tunnel," NASA TM 100883, March 1987.

Janardan, B. A., Chuang, S., Ho, P. Y., and Lee, R., "Scale Model Acoustic Testing of Counterrotating Fans," AIAA 1988-2057, AIAA 15th Aerodynamic Testing Conference, San Diego, CA, May 1988.

Swallow, R. J. and Aiello, R. A., "NASA Lewis 8x6 Foot Supersonic Wind Tunnel," NASA TMX-71542, May 1974.

Woodward, R. P., "Noise of Two High Speed Model Counter-rotation Propellers at Takeoff/Approach Conditions," *Journal of Aircraft*, Vol. 29, No. 4, July/Aug 1992.

Woodward, R. P., Hall, D. G., Podboy, G. G., and Jeracki, R. J., "Takeoff/Approach Noise for a Model Counter-rotation Propeller with a Forward-Swept Upstream Rotor," AIAA 1993-0596, 31st Aerospace Sciences Meeting, Reno, NV, January 1993.

Yuska, J. A., Diedrich, J. H., and Clough, N., "Lewis 9x15 Foot V/STOL Wind Tunnel," NASA TMX-2305, July 1971.